

Thermodynamic properties and phase equilibria in Na<sub>2</sub>O-SiO<sub>2</sub> and K<sub>2</sub>O-SiO<sub>2</sub> Systems.

A.A.Tsaplin, A.I.Zaitsev, N.E.Shelkova and B.M.Mogutnov

Institute for Metal Physics and Functional Materials, I.P.Bardin Central Research Institute for  
Ferrous Metallurgy

9/23 2-nd Baumanskaya Ul., Moscow 107005, Russia

### **Abstract.**

Knudsen effusion mass spectrometry and the method based on generation in the effusion cell of reduction reactions producing volatile suboxides were used to study the thermodynamic properties of the Na<sub>2</sub>O-SiO<sub>2</sub> and K<sub>2</sub>O-SiO<sub>2</sub> systems in solid and liquid states. Nb, Ta, Mo, Ni or Al served as reducers. K<sup>+</sup>, K<sub>2</sub>O<sup>+</sup>, KO<sup>+</sup>, Na<sup>+</sup>, Na<sub>2</sub>O<sup>+</sup>, NaO<sup>+</sup>, O<sub>2</sub><sup>+</sup>, MO<sup>+</sup>, MO<sub>2</sub><sup>+</sup> (M=Nb, Ta, Mo), MoO<sub>3</sub><sup>+</sup>, NiO<sup>+</sup> and Al<sub>2</sub>O<sup>+</sup> were detected in the mass spectra of the saturated vapour over the K<sub>2</sub>O-SiO<sub>2</sub> and Na<sub>2</sub>O-SiO<sub>2</sub> compositions. K, Na, TaO<sub>2</sub>, NbO<sub>2</sub>, MoO<sub>2</sub>, NiO, Al<sub>2</sub>O, KO<sub>2</sub> and NaO<sub>2</sub> were found to be the main vapour species and their partial vapour pressures were measured and used for calculation of  $a(\text{K}_2\text{O})$  and  $a(\text{Na}_2\text{O})$ . The activity of SiO<sub>2</sub> was calculated using the Gibbs-Duhem equation. The Gibbs energies of formation of solid potassium and sodium silicates were found. The thermodynamic functions of the liquid solutions were described by the associated-solution model under the assumption that binary associates and SiO<sub>2</sub> polymer complexes exist in the melts. The model and the thermodynamic functions of solid compounds were applied for the computation of the phase diagram. The computed co-ordinates of the invariant points are shown to agree with the available experimental data.

### **1. Introduction.**

Sodium and potassium silicates form a part of numerous minerals, so that the thermodynamic properties of the Na<sub>2</sub>O-SiO<sub>2</sub> and K<sub>2</sub>O-SiO<sub>2</sub> systems are of great interest for various branches of earth science. They are also important for development of new technologies in metallurgy, in production of ceramics, glass and refractories. Theoretical interest to thermodynamics of molten alkali silicates is connected with the unique capacity of SiO<sub>2</sub> for polymerisation as well as with the very intensive heteromolecular interactions. The former results in formation of silicon dioxide molecules of various size and spatial configuration, the latter leads to extremely low values of the component activities. All attempts to describe the thermodynamic properties of the liquid alkali silicates in the context of the widely spread ionic-solution concept of their structure have failed, although these melts seem to be almost ideal ionic solution (see, for example, Refs [1-4]). The most probable cause of the failure is inadequate

simplified treatment of  $\text{SiO}_2$  polymerisation reaction. Shakhmatkin and Shults [5] have shown that in the case of the  $\text{Na}_2\text{O-SiO}_2$  liquid solution the best result to be expected from consideration of the  $\text{O}^0 + \text{O}^{2-} = 2\text{O}^{1-}$  equilibrium is qualitative agreement with experimental thermodynamic data.

An alternative way of approximation of molten silicates thermodynamic properties [6-8] has been developed in recent years. It is founded on Prigogine's associated-solution theory [9] and proceeds from assumption that the structure species are molecules of the components, heteromolecular associates and  $\text{SiO}_2$  polymer complexes, the equilibrium constant of the addition of any  $\text{SiO}_2$  molecule to a silicon dioxide polymer complex being independent on either its size or its configuration. This approach has succeeded in description of several systems of various complexities:  $\text{MnO-SiO}_2$  [6],  $\text{CaO-SiO}_2$ , [7],  $\text{Al}_2\text{O}_3\text{-SiO}_2$ ,  $\text{CaO-Al}_2\text{O}_3\text{-SiO}_2$ , and  $\text{CaO-Al}_2\text{O}_3\text{-SiO}_2\text{-CaF}_2$  [8]. It seems worth to put the associated-solution model to a test and apply it to the liquid  $\text{Na}_2\text{O-SiO}_2$  and  $\text{K}_2\text{O-SiO}_2$  solutions, where deviations from the Raoult's law are remarkably high and the components' activity coefficients reach the values of  $10^{-8}$  to  $10^{-11}$ . Therein lies the main purpose of this work. Some preconditions of the success can be found in refs. 5 and 10. As a matter of fact the authors of this works has shown that the associated-solution theory leads to qualitative agreement with experiment even under a simple and rather inadequate assumption that all sodium or potassium oxide is bonded in the  $\text{Na}_2\text{O} \cdot \text{SiO}_2$  and  $\text{Na}_2\text{O} \cdot 2\text{SiO}_2$  or  $\text{K}_2\text{O} \cdot \text{SiO}_2$ ,  $\text{K}_2\text{O} \cdot 2\text{SiO}_2$  and  $\text{K}_2\text{O} \cdot 4\text{SiO}_2$  associative complexes.

The test requires reliable thermodynamic information on both liquid and solid silicates, but the available data are fragmentary and rather contradictory. For example, the data on  $a(\text{Na}_2\text{O})$  reported in refs [1,2,4,5,11-22] differ by several orders of magnitude. In considerable part of the studies of molten potassium silicates [11,12,23] only relative values of  $\text{K}_2\text{O}$  activities were determined and the results of the other works [10,21,24,25] differ more than by a factor of 40. Knowledge of solid silicates is significantly worse. Only part of them was studied experimentally, the thermodynamic properties of the others are based on estimations [26-28]. That is why the second purpose of this work is to determine the thermodynamic properties of solid and liquid phases in the  $\text{Na}_2\text{O-SiO}_2$  and  $\text{K}_2\text{O-SiO}_2$  systems.

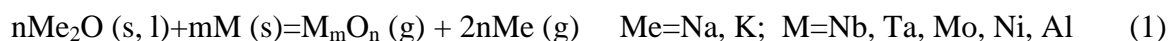
## 2. Experimental.

Samples were prepared from high purity silicon dioxide calcined under vacuum and sodium or potassium oxide obtained by decomposition of corresponding carbonates of high-purity

grade. One part of them was synthesised directly in effusion cells under a pressure of  $< 10^{-4}$  Pa and the other was smelted in closed nickel crucibles also under the same pressure. In order to prevent hydrolysis of the smelted samples, all manipulations with them were carried out in a box under an atmosphere of dry nitrogen.

Knudsen effusion mass spectrometry and the method [6,8] based on generation in the effusion cell of reduction reactions producing volatile suboxides were chosen in the present work for the experimental study. Niobium, tantalum, molybdenum, nickel, or aluminium served as reducers. The first four were used as cell materials and in some experiments powder of these metals as well as powder of aluminium was mixed with the test substances. Random sampling showed that the concentration of the reducer oxides in these substances after the experiments was insignificant ( $< 0.05\%$ ). Double effusion cells were used in experiments. Silver (99.99 %), nickel (99.98 %), or copper (99.999%) was used as references substances. The temperature functions of the ion currents (vapour pressures) of these substances were well reproducible in all cases, and were in good agreement with the thermodynamic databank IVTANTERMO [29]. The vapour pressures of the reference substances from this source were used in the calculations. In order to control the state of equilibrium in the effusion cell, the cell diameter was varied and the samples of the same composition were studied in the cells made from different materials. The conditions of the experiments were such that the changes in composition of samples occurring because of evaporation were insignificant and could be neglected. The experimental procedure was the same as reported earlier [30,31].

$K^+$ ,  $K_2O^+$ ,  $KO^+$ ,  $Na^+$ ,  $Na_2O^+$ ,  $NaO^+$ ,  $O_2^+$ ,  $MO^+$ ,  $MO_2^+$  ( $M=Nb, Ta, Mo$ ),  $MoO_3^+$ ,  $NiO^+$  and  $Al_2O^+$  were detected in the mass spectra of the saturated vapour over the  $K_2O-SiO_2$  and  $Na_2O-SiO_2$  compositions. They evidently originated from ionisation of  $K$ ,  $K_2O$ ,  $KO$ ,  $KO_2$ ,  $Na$ ,  $Na_2O$ ,  $NaO$ ,  $NaO_2$ ,  $O_2$ ,  $MO$ ,  $MO_2$  ( $M=Nb, Ta, Mo$ ),  $MoO_3$ ,  $NiO$  and  $Al_2O$ . The  $K^+$ ,  $Na^+$ ,  $TaO_2^+$ ,  $NbO_2^+$ ,  $MoO_2^+$ ,  $NiO^+$  and  $Al_2O^+$  peaks were the most intensive and the  $O_2^+$  lines were registered only in experiments with  $Mo$  or  $Ni$  cells. No peaks connected with the products of reduction of silicon dioxide were detected in the mass spectra, so that only alkali oxides were reduced in the experiments according to the reaction:



As in all cases  $a(M)=1$ , this reaction allowed calculation of the activity of the alkali oxides from the vapour pressures (ion currents,  $I$ ) measured over compositions saturated and unsaturated with  $Na_2O$  or  $K_2O$  using the following equation:

$$[a(\text{Me}_2\text{O})]^n = \frac{p(\text{M}_m\text{O}_n)[p(\text{Me})]^{2n}}{p^o(\text{M}_m\text{O}_n)[p^o(\text{Me})]^{2n}} = \frac{I(\text{M}_m\text{O}_n^+)[I(\text{Me}^+)]^{2n}}{I^o(\text{M}_m\text{O}_n^+)[I^o(\text{Me}^+)]^{2n}}, \quad (2)$$

where the values with the superscript ‘o’ refer to the liquid of  $a(\text{Me}_2\text{O})$  equal to unity.

Assignment of the lines connected with ionisation Nb, Ta, Mo, Al and Ni oxides followed the scheme proposed in ref. [6,7, 32,33] and that of the  $\text{K}^+$ ,  $\text{K}_2\text{O}^+$ ,  $\text{KO}^+$ ,  $\text{Na}^+$ ,  $\text{Na}_2\text{O}^+$ ,  $\text{NaO}^+$ ,  $\text{O}_2^+$  lines is described in the paper presented at this conference by A.I.Zaitsev [34].

### 3. Results.

#### 3.1. Liquid solution.

A representative files of experimental data comprising about 550 values of  $a(\text{Na}_2\text{O})$  and 350 values of  $a(\text{K}_2\text{O})$  at various temperatures and/or concentrations were obtained here. The activities computed from the data obtained under different experimental conditions in the effusion cells of different diameter, were in good agreement. Divergence never exceeded 1-3 per cent. Activities of  $\text{SiO}_2$  were calculated by integration of the Gibbs-Duhem equation, using  $\alpha$ -function:  $\alpha(\text{Me}_2\text{O}) = \ln \gamma(\text{Me}_2\text{O}) / [1 - x(\text{Me}_2\text{O})]^2$ . The co-ordinates of the points on the phase diagram that described saturation of the liquid solution with  $\text{SiO}_2$  were required for the integration. They were assumed to coincide with the co-ordinates of the points where the  $(\text{Me}_2\text{O})$  vs. concentration curves became horizontal. The values found in this way were subsequently checked in the process of computation of the phase diagram (see paragraph “Phase equilibria”). In no case did the results of the two determinations differ substantially. The following data illustrate this fact.

System	$\text{Na}_2\text{O-SiO}_2$	$\text{K}_2\text{O-SiO}_2$
$T, \text{K}$	1473	1373
$x(\text{SiO}_2)$ at from exp. data	0.805	0.860
saturation From phase diagram	0.808	0.857

Some values of activity chosen at random are given in Table 1.

#### 3.2. Solid compounds.

All solid sodium compounds and three potassium silicates,  $\text{K}_2\text{O} \cdot 4\text{SiO}_2$ ,  $\text{K}_2\text{O} \cdot 2\text{SiO}_2$ ,  $\text{K}_2\text{O} \cdot \text{SiO}_2$ , were studied in this work. Several samples of different composition belonging to each field of the two-phase equilibria as well as stoichiometric compounds  $\text{Na}_2\text{O} \cdot \text{SiO}_2$  and  $2\text{Na}_2\text{O} \cdot \text{SiO}_2$  were used for the vapour pressure measurements. Pure  $\beta\text{-Na}_2\text{O}$ , solid  $\text{K}_2\text{O}$  and  $\text{SiO}_2$  were chosen as the standard states and the data of the IVTANTERMO databank [29] were used to convert the measured values to these states.  $\Delta G(\text{Me}_2\text{O})$  values, found in experiments with effusion cells of different materials and various orifice areas and in

experiments with samples of different composition in the same heterogeneous region, were in good agreement.

To determine partial enthalpies and entropies of  $\text{Me}_2\text{O}$  the discussed experimental data were approximated by the linear function,  $\Delta G(\text{Me}_2\text{O}) = \Delta H(\text{Me}_2\text{O}) + T \times \Delta S(\text{Me}_2\text{O})$ , using the least-squares method. Calculations of the integral thermodynamic functions of solid silicates were carried out by means of the Gibbs-Duhem equation, where integration was replaced by summation. The results of calculations are given in Table 2.

#### 4. The Associated-Solution Model of $\text{Na}_2\text{O-SiO}_2$ and $\text{K}_2\text{O-SiO}_2$ Melts.

The associated solution model [6-8] of silicate melts is based on consideration of two concurrent processes: polymerisation of silicon dioxide and formation of heteromolecular complexes. The previous results show that in binary molten silicates the number of types of heteromolecular complexes depends on the basicity of the second oxide, increasing from a single associate  $\text{Al}_2\text{O}_3 \cdot \text{SiO}_2$  in the  $\text{Al}_2\text{O}_3\text{-SiO}_2$  [8], to two associates  $2\text{MnO}(\text{CaO}) \cdot \text{SiO}_2$  and  $\text{MnO}(\text{CaO}) \cdot \text{SiO}_2$  in  $\text{MnO-SiO}_2$  [6] and  $\text{CaO-SiO}_2$  [7,8]. Intensification of the acidic-basic interaction leads not only to formation of new heteromolecular complexes, but also to bonding of some complexes to silicon-oxygen networks [8]. The latter was observed by adding  $\text{Al}_2\text{O}_3$  to  $\text{CaO-SiO}_2$  and  $\text{CaF}_2\text{-CaO-SiO}_2$ . The present experimental data show that the interparticle interaction in the liquid alkali silicates studied is significantly stronger than that in the systems considered above. Thus, it seems safe to suppose that  $\text{N}_2\text{S}$  and  $\text{NS}$  or  $\text{K}_2\text{S}$  and  $\text{KS}$  associates exist in the liquid  $\text{Na}_2\text{O-SiO}_2$  or  $\text{K}_2\text{O-SiO}_2$  (hereafter N denotes  $\text{Na}_2\text{O}$ , K -  $\text{K}_2\text{O}$  and S -  $\text{SiO}_2$ ) and that the silicon dioxide polymer structures can be connected with the NS (KS) associates to form  $\text{N(K)S}_j$  ( $2 \leq j \leq \infty$ ) networks. However, the congruently melting compounds correspond to the complexes  $\text{NS}_2$  and  $\text{KS}_2$ . Therefore it is preferable to single out these complexes from  $\text{N(K)S}_j$  networks and consider them as individual associates. This means that the associated-solution species of the melts under consideration are molecules of the components or monomers  $\text{N}_1$ ,  $\text{K}_1$  and  $\text{S}_1$ ; complexes  $\text{Na}_2\text{S}$ ,  $\text{NaS}$ ,  $\text{NaS}_2$ ,  $\text{K}_2\text{S}$ ,  $\text{KS}$ ,  $\text{KS}_2$ ; silicon dioxide networks of various configurations and size ( $\text{S}_k$ ,  $2 \leq k \leq \infty$ );  $\text{SiO}_2$  networks connected with  $\text{NaS}_2$ ,  $\text{KS}_2$  ( $\text{NS}_j$ ,  $\text{KS}_j$ ,  $3 \leq j \leq \infty$ ). In accordance with the results of ref. 6-8, we will assume that the equilibrium constant of the addition of an  $\text{SiO}_2$  molecule to any oxygen-silicon network  $\text{S}_k$ ,  $\text{NS}_j$  or  $\text{KS}_j$  at  $j \geq 3$  depends on neither the size nor the configuration of the complex and is equal to the equilibrium constant,  $K_p$ , of the reaction  $\text{S}_1 + \text{S}_1 = \text{S}_2$ . The thermodynamic characteristics of the last reaction are expected to coincide with those found for  $\text{MnO-SiO}_2$ ,  $\text{CaO-SiO}_2$ ,  $\text{Al}_2\text{O}_3\text{-SiO}_2$ ,  $\text{CaO-Al}_2\text{O}_3\text{-SiO}_2$  and  $\text{CaF}_2\text{-CaO-Al}_2\text{O}_3\text{-SiO}_2$ .

solutions. In the associated-solution theory, the activities of the components are to be obtained by multiplying the mole fractions of the monomer species and the corresponding activity coefficients. The former can be calculated by solving the system of equations that connect the mole fractions of the components with those of the associated-solution species and originate from the conservation of mass. The latter are to be found from the equation for the excess Gibbs energy. All necessary formulae of the model are described in details in previous publications [6-8] and partly are given in the paper [35], presented at this conference.

The optimisation procedure [6] was applied to the whole files of data on the components' activities in the Na<sub>2</sub>O-SiO<sub>2</sub> and K<sub>2</sub>O-SiO<sub>2</sub> melts in order to establish the thermodynamic characteristics of the association and polymerisation reactions and the parameters describing the excess Gibbs energy. Although the thermodynamic characteristics of SiO<sub>2</sub> polymerisation were determined in previous studies, at the first optimisation stage they were assumed unknowns. Consequently, it was found that the enthalpy of the silica polymerisation process,  $\Delta H_p$ , is equal to  $-92750 \text{ J mol}^{-1}$  for K<sub>2</sub>O-SiO<sub>2</sub> solution and to  $-92370 \text{ J mol}^{-1}$  for Na<sub>2</sub>O-SiO<sub>2</sub>. The entropy of this reaction,  $\Delta S_p$ , was found equal to  $-27.4 \text{ J mol}^{-1} \text{ K}^{-1}$  and  $-27.1 \text{ J mol}^{-1} \text{ K}^{-1}$ . These values coincide, within experimental error, with the values established in refs 6-8. For this reason, at the second stage of optimisation,  $\Delta H_p$  and  $\Delta S_p$  were assumed equal to those obtained previously. This did not lead to significant changes in the other thermodynamic characteristics. As the result of the computations, it was proven that the associated-solution model approximated the experimental data with a precision not worse than the experimental one (2-3 %), if the free parameters had the following values:

$$\begin{aligned}
 \Delta H_p &= -92575 \text{ J mol}^{-1} & \Delta S_p &= -27.2 \text{ J mol}^{-1} \text{ K}^{-1} \\
 \Delta_f H (\text{NS}) &= -322830 \text{ J mol}^{-1} & \Delta_f S (\text{NS}) &= -32.5 \text{ J mol}^{-1} \text{ K}^{-1} \\
 \Delta_f H (\text{N}_2\text{S}) &= -520580 \text{ J mol}^{-1} & \Delta_f S (\text{N}_2\text{S}) &= -81.3 \text{ J mol}^{-1} \text{ K}^{-1} \\
 \Delta_f H (\text{NS}_2) &= -433220 \text{ J mol}^{-1} & \Delta_f S (\text{NS}_2) &= -55.5 \text{ J mol}^{-1} \text{ K}^{-1} \\
 \Delta_f H (\text{KS}) &= -386200 \text{ J mol}^{-1} & \Delta_f S (\text{KS}) &= -61.9 \text{ J mol}^{-1} \text{ K}^{-1} \\
 \Delta_f H (\text{K}_2\text{S}) &= -634000 \text{ J mol}^{-1} & \Delta_f S (\text{K}_2\text{S}) &= -89.3 \text{ J mol}^{-1} \text{ K}^{-1} \\
 \Delta_f H (\text{KS}_2) &= -492000 \text{ J mol}^{-1} & \Delta_f S (\text{KS}_2) &= -54.7 \text{ J mol}^{-1} \text{ K}^{-1} \\
 L_{11} &= 24920 \text{ J} & L_{22} &= -119040 \text{ J in Na}_2\text{O-SiO}_2 \text{ melt} \\
 L_{11} &= -31300 + 20.0 \cdot T \text{ J} & L_{22} &= -139000 + 62.0 \cdot T \text{ J in K}_2\text{O-SiO}_2 \text{ melt}
 \end{aligned} \tag{7}$$

Table I, where the calculated component activities are compared with the experimental data, illustrates the validity of the model. It is seen that the differences between the two-type values do not exceed the experimental error (1-3%). Thus, in contrast to the ionic-solution concept

the associate solution model describes well the thermodynamic properties of molten alkali silicates.

Besides, the models [1-5,10] mentioned above there is one more approach that represents the temperature and concentration functions of the components' activities in the  $\text{Na}_2\text{O-SiO}_2$  and  $\text{K}_2\text{O-SiO}_2$  solutions correctly enough. This is the "structureless" modified quasichemical model [36,37] that treats the melt as a short-range ordered liquid. It considers only the distribution of cations on the cationic quasi-lattice under assumption that the concentration dependencies of enthalpy and non-configuration entropy, connected with the ordering process, can be approximated by polynomials of up to seventh degree. The parameters of the model were determined by optimisation of the experimental data on the thermodynamic properties and phase equilibria. However, as it will be shown below, it gives a worse description of the phase diagrams.

## 5. Discussion.

### 5.1. Alkali oxide activity in the melts.

The composition dependence of  $\text{Na}_2\text{O}$  activity in the melt is given in Fig. 1 in comparison with available data [1,2,4,5,11-16,18,20,21]. The authors of ref. 12 and 13 reported  $a(\text{Na}_2\text{O})$  with respect to the solution with the mole fraction of silicon dioxide equal to 0.67 and 0.6, correspondingly. To reduce these data to the standard state, pure liquid  $\text{Na}_2\text{O}$ , accepted here, the present  $a(\text{Na}_2\text{O})$  values for the above concentrations were used. One can see that there is good agreement between the present results and the data obtained by EMF measurements [1,4,5,12-14] and by studying heterogeneous equilibria [18]. The values  $a(\text{Na}_2\text{O})$ , reported in ref. 2, 20, 21, are somewhat higher than the present results. In the first the Na vapour pressure over the  $\text{Na}_2\text{O-SiO}_2$  liquid solution, equilibrated with graphite under a certain  $p(\text{CO})$ , was measured, using the transport technique. In the other two the Knudsen mass spectrometry was applied. The cause of disagreement is evidently the complexity of the mechanism of  $\text{Na}_2\text{O}$  vaporisation [34,38], which was unknown when the experiments [2,20,21] were carried out. Formation of silicon carbide was also quite possible in experiments [2]. Dissolving in the silicate melt this compound could, of course, influence  $a(\text{Na}_2\text{O})$ . It should be noted here that though  $a(\text{Na}_2\text{O})$  reported by Tsukihashi and Sano [18] are in general agreement with the present results the partial enthalpy and entropy of  $\text{Na}_2\text{O}$  diverge. More than that, the reverse concentration behaviour of  $\Delta S(\text{Na}_2\text{O})$  was found in ref. 18, which is in obvious contradiction with the nature of structural changes occurring when a basic oxide is added to the silicon dioxide melt (see below). This disagreement can be explained by the narrowness of the temperature range studied in ref. 18 that did not allow an accurate determination of the

temperature dependence of  $a(\text{Na}_2\text{O})$ . The results of the research of ion-molecular equilibria [22] (not shown in Fig.1) also agree with the present  $a(\text{Na}_2\text{O})$ . Fig. 1 shows that extremely low value  $a(\text{Na}_2\text{O})$  are inherent in the  $\text{Na}_2\text{O}-\text{SiO}_2$  liquid solution. They grow rapidly as temperature rises. The latter means that the absolute value of  $\text{Na}_2\text{O}$  partial enthalpy is rather high. Similar regularity was found in all previous works except [15,16] where the inverse one was observed. It should be emphasised that the data [15,16] differ sharply from the results of all other investigations.

The composition dependence of  $\text{K}_2\text{O}$  activity in the melt is given in Fig. 2 in comparison with available data. The authors of [11,12,23] reported only relative values of  $a(\text{K}_2\text{O})$  obtained with respect to the solution with the mole fraction of silicon dioxide equal to 0.744, 0.66 or 0.667, correspondingly. To reduce these data to the standard state, pure liquid  $\text{K}_2\text{O}$ , accepted here, the present  $a(\text{K}_2\text{O})$  values for the above concentrations were used. One can see from Fig. 2 that the present results agree with the EMF data [10-12,23] in magnitude, but somewhat differ in the form of concentration functions. It is quite possible that this difference is connected with uncertainties in the nature of the electrode reaction discussed in ref. 39. Some confirmation of this suggestion can be found in the following fact. According to [10,12] the curves, describing  $a(\text{K}_2\text{O})$  versus  $x(\text{SiO}_2)$  functions in the concentration interval  $0.5 \leq x(\text{SiO}_2) \leq 0.8$  and temperature range 973-1273 K, are smooth like in homogeneous solution. However, it is known that the melting point of potassium disilicate is equal to 1318 K [37,40,41] and in reality the above mixtures should be two phase. The data of the two mass spectrometric studies [21,24] are also in general agreement with the present  $a(\text{K}_2\text{O})$  values. The differences can be apparently connected to some extent with the complexity of the mechanism of alkali oxides vaporisation mentioned above. However, the method used by Plante [24] suggests that there were other sources of discordance. Indeed, this author estimated the accuracy of temperature measurements as  $\pm 20$  centigrade and that of composition determinations as  $\pm 2\%$  at the beginning of the experiments and  $\pm 5\%$  at the end. The uncertainty in temperature alone could lead to an error of  $\sim 40\%$  in potassium vapour pressure measurements at 1500 K. Besides, Plante calibrated the mass spectrometer by means the integral method, assuming that the sensitivity constant remained unchanged throughout the experiment and could be determined at the end of it by the loss of the sample weight. Some evidences of Plante's method weakness can be found in the work [24] itself. It suffices to mention disagreement in the results obtained in the effusion cells of different orifice diameter. Further still, there was disagreement between the results obtained by mass



spectrometry and by continuous weighing of the effusion cell. The heterogeneous equilibria technique [25] resulted in the  $a(\text{K}_2\text{O})$  values that are close to the present data both in magnitude and in the form of concentration function. Some distinction can be observed only between temperature dependences, which is quite understandable. Indeed, owing to many possible side reactions that might occur in the experiments [25], accurate determination of the  $a(\text{K}_2\text{O})$  *versus* temperature curves seems to be very difficult. Besides the experimental studies discussed there is one more work [42] where  $a(\text{K}_2\text{O})$  values were estimated using the coordinates of the liquidus line at the phase diagram [40], data on volatility of the  $\text{K}_2\text{O}$ - $\text{SiO}_2$  melt [43] and the Gibbs energy of formation of potassium disilicate [44]. Fig. 2 shows that the estimations [42] are in agreement with present results.

### 5.2. $\text{SiO}_2$ activity in the melts.

Isotherms of the concentration dependence of  $a(\text{SiO}_2)$  in comparison with the literature data are given in Fig. 3 and 4. They are seen to intersect at  $x(\text{SiO}_2) \approx 0.3$  in  $\text{Na}_2\text{O}$ - $\text{SiO}_2$  and at  $x(\text{K}_2\text{O}) \approx 0.225$  in  $\text{K}_2\text{O}$ - $\text{SiO}_2$  indicating a change of sign of  $\text{SiO}_2$  partial enthalpy, from positive for  $\text{SiO}_2$ -rich melt to negative for alkali oxide-rich melt. A similar intersection was found in the  $\text{CaO}$ - $\text{SiO}_2$  solution at  $x(\text{SiO}_2) \approx 0.6$  [7] and in the  $\text{MnO}$ - $\text{SiO}_2$  one at  $x(\text{SiO}_2) \approx 0.68$  [6]. The change of sign can evidently be explained by the structural changes occurring when basic oxides are added to liquid  $\text{SiO}_2$ . In  $\text{SiO}_2$ -based solutions, the gain in enthalpy connected with formation of bonds between basic oxides and  $\text{SiO}_2$  is lower than the loss in enthalpy accompanying destruction of  $\text{SiO}_2$  polymer networks. At high basic oxides concentrations the polymer networks are mostly destroyed so that the gain in enthalpy connected with formation of bonds between these oxides and  $\text{SiO}_2$  is dominating. The regularity in alteration of the intersection point co-ordinate in the series:  $\text{K}_2\text{O}$ ,  $\text{Na}_2\text{O}$ ,  $\text{CaO}$ ,  $\text{MnO}$ , reflects the changes in basicity of the oxide and, correspondingly, in the energy of its interaction with  $\text{SiO}_2$ .

All  $a(\text{SiO}_2)$  concentration dependencies in Fig. 3 and 4 were obtained through the Gibbs-Duhem equation. One can see from Fig. 3 that in case of  $\text{Na}_2\text{O}$ - $\text{SiO}_2$  there is good agreement between the present isotherms and the curve calculated from the results of studying heterogeneous equilibria [18]. The data obtained through EMF measurements [1,4] also agree with the present isotherms. Some differences between various sources can be attributed to the differences in the initial points of integration, *i.e.* in the co-ordinates of the line of saturation of the liquid solution with  $\text{SiO}_2$ . Note that in the present work these co-ordinates, found with the help of the  $a(\text{Na}_2\text{O})$  *vs.* concentration function, were verified in subsequent computation

of the phase diagram (see below). In case of  $\text{K}_2\text{O}\text{-SiO}_2$  (Fig. 4) there is agreement, within the experimental uncertainties, between the present isotherms and the curves reported by Charles [42] and Kozhina [10]. The concentration dependence of  $a(\text{SiO}_2)$  found in [11] is totally different. The disagreement can be attributed to the causes discussed above while considering  $a(\text{K}_2\text{O})$ .

### 5.3. Solid Silicates.

The thermodynamic functions of solid silicates at high temperatures were obtained in the present study for the first time. The available thermodynamic description of sodium and potassium meta- and disilicates as well as the information on sodium orthosilicate [26-28] is founded on calorimetric measurements of the formation enthalpies and low-temperature heat capacities. With regard to the potassium tetrasilicate and the other two sodium compounds, only assessment of their thermodynamic properties carried out by optimisation of the thermodynamic and phase equilibria data is available in the literature [26,37]. For comparison of the present results with literature data, the standard thermodynamic functions of the solid silicates were calculated, using the values given in Table 2, the compounds' heat capacities [26,45,46] and thermodynamic functions of the components:  $\text{SiO}_2$  [47],  $\text{Na}_2\text{O}$  [29] and  $\text{K}_2\text{O}$  [27,29]. The results are given in Table 3 together with values recommended in [26-28]. The uncertainties of the standard thermodynamic functions found here include all sources of error: statistical scattering (see Table 2), inaccuracies in ionisation cross-sections and measurement of temperature, ionic currents and orifice areas.

One can see that the present results on sodium silicates agree, within the limit of experimental errors, with recommendations [26]. Estimations [37] of the  $3\text{Na}_2\text{O}\cdot 8\text{SiO}_2$  and  $3\text{Na}_2\text{O}\cdot 2\text{SiO}_2$  properties are also in reasonable agreement with present results. The present data on  $\text{K}_2\text{O}\cdot \text{SiO}_2$  and  $\text{K}_2\text{O}\cdot 2\text{SiO}_2$  also agree, within the limits of experimental error, with recommendations [27,28]. Knacke *et al.* [26] give a lower value for the formation enthalpy of metasilicate and somewhat higher value for the absolute entropy of disilicate, though in the last case the difference is hardly significant. The last source gives somewhat higher value for the formation enthalpy of potassium tetrasilicate, but the difference in the absolute entropy between the present value and recommendation [26] seems insignificant. The agreement in the formation and absolute entropies of the crystalline silicates seems to be most important because in the previous studies these characteristics were based on the third law of thermodynamics.

### 5.4. Phase Diagrams.

The present model of the  $\text{Na}_2\text{O-SiO}_2$  and  $\text{K}_2\text{O-SiO}_2$  melts and the thermodynamic functions of solid silicates have been applied for the computation of the phase diagrams. The Gibbs energies of phase transitions were chosen from [29] for  $\text{Na}_2\text{O}$ ,  $\text{K}_2\text{O}$  and from [47] for  $\text{SiO}_2$ . The computation was carried out by the chemical equipotentials method. All possible phase combinations were analysed. The combinations, corresponding to the highest changes of the Gibbs energies, were considered to be in equilibrium and their characteristics were applied for construction of the phase diagrams. All others were considered metastable and their characteristics were ignored. The computed phase diagrams together with the results of the experimental determination of the line of saturation of the  $\text{Na}_2\text{O-SiO}_2$  liquid solution with  $\text{SiO}_2$  and the co-ordinates of the particular points [40,48-52] are shown in Fig. 5 and 6. On the whole, agreement between the computed and the experimental phase diagrams is seen to be quite good. The discrepancies, as a rule, do not exceed a few K in temperature and a few thousandths in mole fraction. In this respect the present model surpasses the modified quasichemical model [36,37], which, according to its authors, approximates the phase equilibria in the  $\text{Na}_2\text{O-SiO}_2$  system with the uncertainty of  $\pm 10^\circ\text{C}$  in general and even  $\pm 50$  centigrade, when  $x(\text{SiO}_2) > 0.75$ .

The calculation results require only a few comments. Sodium orthosilicate was found [48,49] to decompose peritectically at 1392 K and to form a eutectic with  $\text{Na}_2\text{O}\cdot\text{SiO}_2$  at  $T=1296$  K and  $x(\text{SiO}_2)=0.438$ . However, the melting point of pure  $\text{Na}_2\text{O}$  is equal to 1405 K [29], there is no intermediate phase between  $\text{Na}_2\text{O}$  and  $2\text{Na}_2\text{O}\cdot\text{SiO}_2$ ,  $2\text{Na}_2\text{O}\cdot\text{SiO}_2$  is the most stable of the sodium silicates. All these facts suggest that incongruent melting of the orthosilicate is quite unlikely. As a matter of fact, the experiments [50,51] revealed that in reality  $2\text{Na}_2\text{O}\cdot\text{SiO}_2$  melted congruently at 1358 K. The authors of these works also discovered  $3\text{Na}_2\text{O}\cdot 2\text{SiO}_2$  which melted at 1397 K and formed eutectics with ortho- and monosilicates at  $T=1275$  K,  $x(\text{SiO}_2)=0.361$  and  $T=1289$  K,  $x(\text{SiO}_2)=0.455$ . Budnikov and Matveev [53] identified one more compound in the  $\text{SiO}_2$ -rich region of the  $\text{Na}_2\text{O-SiO}_2$  phase diagram. They suggested that its stoichiometry corresponded to  $\text{Na}_2\text{O}\cdot 3\text{SiO}_2$ , but the careful X-ray diffraction research [52] revealed that the real composition was  $3\text{Na}_2\text{O}\cdot 8\text{SiO}_2$ . This compound decomposed peritectically to quartz and sodium disilicate at 973 K and melted incongruently at 1082 K, transforming to quartz and liquid. However the  $x(\text{SiO}_2)$  co-ordinate of the eutectics, first from the  $\text{SiO}_2$  site, found in [48,50], contradicted this type of  $3\text{Na}_2\text{O}\cdot 8\text{SiO}_2$  melting. The contradiction was resolved by the present results showing that the incongruent melting of  $3\text{Na}_2\text{O}\cdot 8\text{SiO}_2$  is accompanied by formation of sodium disilicate.

A metastable miscibility gap in the liquid phase was observed in the SiO<sub>2</sub>-rich subsolidus part of the Na<sub>2</sub>O-SiO<sub>2</sub> phase diagram [54-60]. The calculated co-ordinates of this region together with the experimental data obtained by studying the opalescence phenomenon are given in Fig. 7. Good agreement between the two-type values can be seen. It is interesting to note that the authors of ref. 60 approximated the temperature - concentration range of the immiscibility gap by the regular solution model choosing Na<sub>2</sub>O•3SiO<sub>2</sub> and (SiO<sub>2</sub>)<sub>8</sub> as the components. Their success can apparently be attributed to the involuntary use of the ideas of the associated-solution concept. Comparison of the data [6,33,41] allows the conclusion that the temperature-concentration range of the immiscibility region narrows in the series: FeO-SiO<sub>2</sub>, MnO-SiO<sub>2</sub>, CaO-SiO<sub>2</sub>, Na<sub>2</sub>O-SiO<sub>2</sub> and in the Na<sub>2</sub>O-SiO<sub>2</sub> melt it exists only in the metastable state. There is no such gap at all in the K<sub>2</sub>O-SiO<sub>2</sub> system [40] and this fact was confirmed by the present calculations. Thus, the existence and size of the immiscibility region in binary silicate systems seem to be connected directly with silica polymerisation and interaction between the basic oxide and SiO<sub>2</sub>. Both phenomena can obviously be described quantitatively by the associated solution model discussed in the present study.

### Acknowledgements

The work was performed with the financial support of the Russian Fund for Basic Research (99-03-32616). We are very grateful to Dr. A.Litvina and I.Lipgart for the help in experiments and preparation of this paper.

### References.

1. K.S.Goto, S.Yamaguchi, and K.Nagata, in Second International Symposium on Metallurgical Slags and Fluxes, ed. H.A.Fine and D.R.Gaskell, publ. Metal. Soc. AIME, New York 1984, p.467.
2. D.N.Rego, G.K.Sigworth, and W.O.Philbrook, Metall. Trans., 1985, **16B**, 313.
3. S.Yamaguchi, and K.S.Goto, Scand. J. Metallurgy, 1984, **13**, 129.
4. D.A.Neudorf, and J.F.Elliott, Metal. Trans., 1980, **11B**, 607.
5. B.A.Shakhmatkin, and M.M.Shults, (Physics and Chemistry of Glass), 1980, **6**,129.
6. A.I.Zaitsev, and B.M.Mogutnov, J. Mater. Chem., 1995, **5**, 1063.
7. A.I.Zaitsev, A.D.Litvina, and B.M.Mogutnov, Neorganicheskie Materialy, 1997, **33**, 76.
8. A.I.Zaitsev, A.D.Litvina, N.P.Lyakishev, and B.M.Mogutnov, J. Chem. Soc. Faraday Trans., 1997, **93**, 3089.
9. I.Prigogine and R.Defay, Chemical Thermodynamics, Longmans Green and Co., London, 1954.

10. E.L.Kozhina, Fyzika I khimiya stekla (Physics and Chemistry of Glass), 1990, **46**, 679.
11. M.G.Frohberg, E.Caung, and M.L.Kapoor, Arch. Eisenhuttenwes., 1973, **44**, 585.
12. D.Ravaine, E.Azandegbe, and J.L.Souquet, Silicates Industries, 1975, **12**, 333.
13. S.Kohsaka, S.Sato, and T.Yokokawa, J. Chem. Thermodynamics, 1979, **11**, 547.
14. S.Yamaguchi, A.Imai, and K.S.Goto, Scand. J. Metallurgy, 1982, **11**, 263
15. M.L.Pearse, J. Amer. Ceram. Soc., 1964, **47**, 342.
16. M.L.Pearse, J. Amer. Ceram. Soc., 1965, **48**, 611.
17. S.Holmquist, J. Amer. Ceram. Soc., 1966, **49**, 467.
18. F.Tsukihashi, and N.Sano, Tetsu to Hagane, 1985, **71**, 815.
19. V.Piacente, and J.Matousek, Silicaty, 1973, **4**, 269.
20. M.M.Shults, V.L.Stolyarova, and G.G.Ivanov, Fizika I Khimiya Stekla (Physics and Chemistry of Glass), 1987, **13**, 168.
21. R.Chastel, C.Bergman, J.Rogez, and L.C.Mathieu, Chemical Geology, 1987, **62**, 19.
22. E.B.Rudny, O.M.Vovk, L.N.Sidorov, V.L.Stolyarova, B.A.Shakhmatkin, and V.I.Rakhimov, Fizika I Khimiya Stekla (Physics and Chemistry of Glass), 1988, **14**, 218.
23. E.Azandegbe, I.Ansara, and J.L.Souquet, C.R. Acad. Sci. Paris, 1973, **276C**, 1248.
24. E.R.Plante, Natl. Bur. Standards Gaithersburg Spec. Publ. 1979, #561, 265.
25. Steiler, J.M., 1982, Comm.Eur. Communities, [Rep.] EUR., **EUR.7820**, 21-1
26. O.Knacke, O.Kubaschewski, and K.Hisselman, Thermochemical Properties of Inorganic Substances, 2nd Edition, Springer-Verlag, Berlin, 1991.
27. JANAF Thermochemical Tables, 3<sup>rd</sup> Edition, J. Phys. Chem. Ref. Data, 1985, **14**.
28. P.J.Spencer, The Thermodynamic Properties of Silicates, Natl. Phys. Lab., Div. Chem. Standards, NPL Rep. Chem. (UK), 1973, **21**.
29. L.V.Gurvitch, Vestnik Akad. Nauk SSSR., 1983, #3, 54.
30. A.I.Zaitsev, N.V.Korolyov, and B.M.Mogutnov, High Temp. Sci., 1990, **28**, 341.
31. A.I.Zaitsev, N.V.Korolyov, and B.M.Mogutnov, Teplofizika Vysokikh Temperatur, 1989, **27**, 465.
32. A.I.Zaitsev, A.D.Litvina, and B.M.Mogutnov, J. Chem. Thermodyn., 1992, **24**, 1039.
33. A.I.Zaitsev, and B.M.Mogutnov, Neorganicheskie Materialy, 1997, **33**, 975.
34. A.I.Zaitsev, Knudsen Cell Mass Spectrometry of Slags and Silicates, this conference.
35. B.M.Mogutnov, A.I.Zaitsev, N.E.Shelkova, and A.D.Litvina, Associated-Solution Approach to Description of Structure and Properties of Molten Slags, this conference.
36. A.D.Pelton, and M.Blander, Metal. Trans., 1986, **17B**, 807.
37. P.Wu, G.Ericsson, and A.D.Pelton, J. Amer. Ceram. Soc., 1993, **76**, 2059.

38. M.Steinberg, and K.Schofield, J. Chem. Phys., 1991, **94**, 3901.
39. Y.Bottinga, D.F.Weill, and P.Richet, in Thermodynamics of Minerals and Melts, ed. Newton,R.C., and Navrotsky,A., Springer-Verlag, 1981, p. 207.
40. F.C.Kracek, N.L.Bowen, and G.W.Morrey, J. Phys. Chem., 1937, **41**, 1183.
41. Schlackenallas, Verlag Stahleisen M.B.H., 1981, Düsseldorf.
42. R.L.Charles, J. Amer. Ceram. Soc., 1967, **50**,631.
43. E.Preston, and W.E.S.Turner, J. Soc. Glass Technol., 1933, **17**, 124.
44. K.K.Kelley, US Bureau of Mines Rept. Invest. #5901, 1962.
45. R.G.Berman, and H.T.Brown, Contrib. Mineral Petrol., 1985, **89**, 168.
46. R.G.Berman, and H.T.Brown, Contrib. Mineral Petrol., 1986, **94**, 262.
47. M.Hillert, B.Sundman, and X.Wang, Metal. Trans., 1990, **21B**, 303.
48. C.Kracek, J. Phys. Chem., 1930, **34**, 1583.
49. F.C.Kracek, J. Amer. Chem. Soc., 1939,, **61**, 2863.
50. J.D'Ans, and J.Loeffler, Z. Anorg. Allgem. Chem., 1930, **191**, 1.
51. J.Loeffler, Glastech. Ber., 1969, **42**, 92.
52. J.Williamson, and F.P.Glasser, Science, 1965, **148**, 1589.
53. P.P.Budnikov, and M.A.Matveev, Doklady Akademii Nauk USSR, 1956, **107**, 547.
54. N.S.Andreev, D.A.Goranov, E.A.Porai-Koshits, and Yu.G.Sokolov, in Stekloobrasnoe sostoyanie, Katalizovannaya kristallizatsiya stecla , Nauka, Leningrad 1963, vol.1, p.46.
55. N.S.Andreev, and V.I.Aver'yanov, in Stekloobrasnoe sostoyanie , Trudy IV Bcecoyuznogo soveshchaniya, Nauka, Moscow-Leningrad, 1965, p.94.
56. J.J.Hammel, in Proccedings VII-th Internat. Congress on Glass, v.1, Institut National du Verre, Charleroi, Belgium, 1966, paper #36.
57. Y.Mariya, D.H.Warrington, and R.W.Douglas, Phys. Chim. Glasses, 1967, **8**, 19.
58. E.A.Porai-Koshits, and V.I.Aver'yanov, J. Non-Cryst. Solids, 1968, **1**, 29.
59. R.J.Charles, Phys. Chem. Glasses, 1969, **10**, 169.
60. W.Haller, D.Blackburn, and J.H.Simmons, J. Amer. Ceram. Soc., 1974, **57**, 120.
61. A.I.Zaitsev and B.M.Mogutnov, Neorganicheskie Materialy, 1997, **33**, 975.

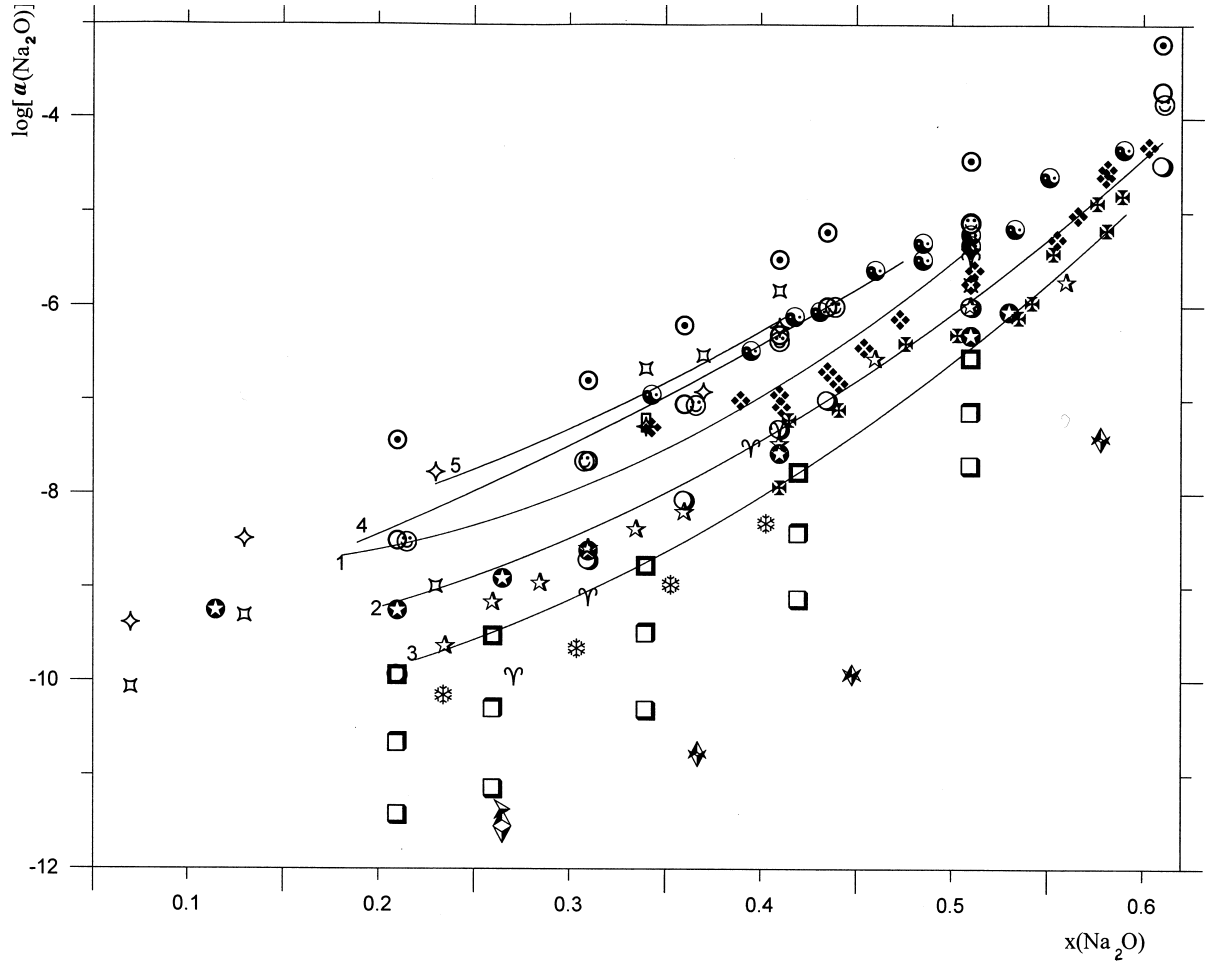


Figure 1. Comparison of  $\text{Na}_2\text{O}$  activities in the  $\text{Na}_2\text{O-SiO}_2$  melt obtained in the present investigation [(1) 1573 K, (2) 1473 K, (3) 1373 K] with the values available in the literature. Ref. [2]: (4) 1573 K, (5) 1673 K; ref. [11]:  $\gamma$  1473 K; ref. [12]:  $\square$  1173K,  $\square$  1273 K,  $\blacksquare$  1373 K; ref.[13]:  $\star$  1450 K; ref. [4]:  $\ast$  1323 K; ref. [5]:  $\odot$  1473 K; ref.[14]:  $\odot$  1473 K; ref.[1]:  $\circ$  1373 K,  $\circ$  1573 K,  $\odot$  1773 K, ref. [15,16]:  $\triangleright$  1273 K,  $\triangle$  1373 K,  $\nabla$  1473 K; ref.[18]:  $\odot$  1573 K,  $\diamond$  1473 K,  $\times$  1373 K, ref. [20]:  $\boxtimes$  1293 K,  $\diamond$  1423 K; ref. [21]:  $\square$  1373 K.

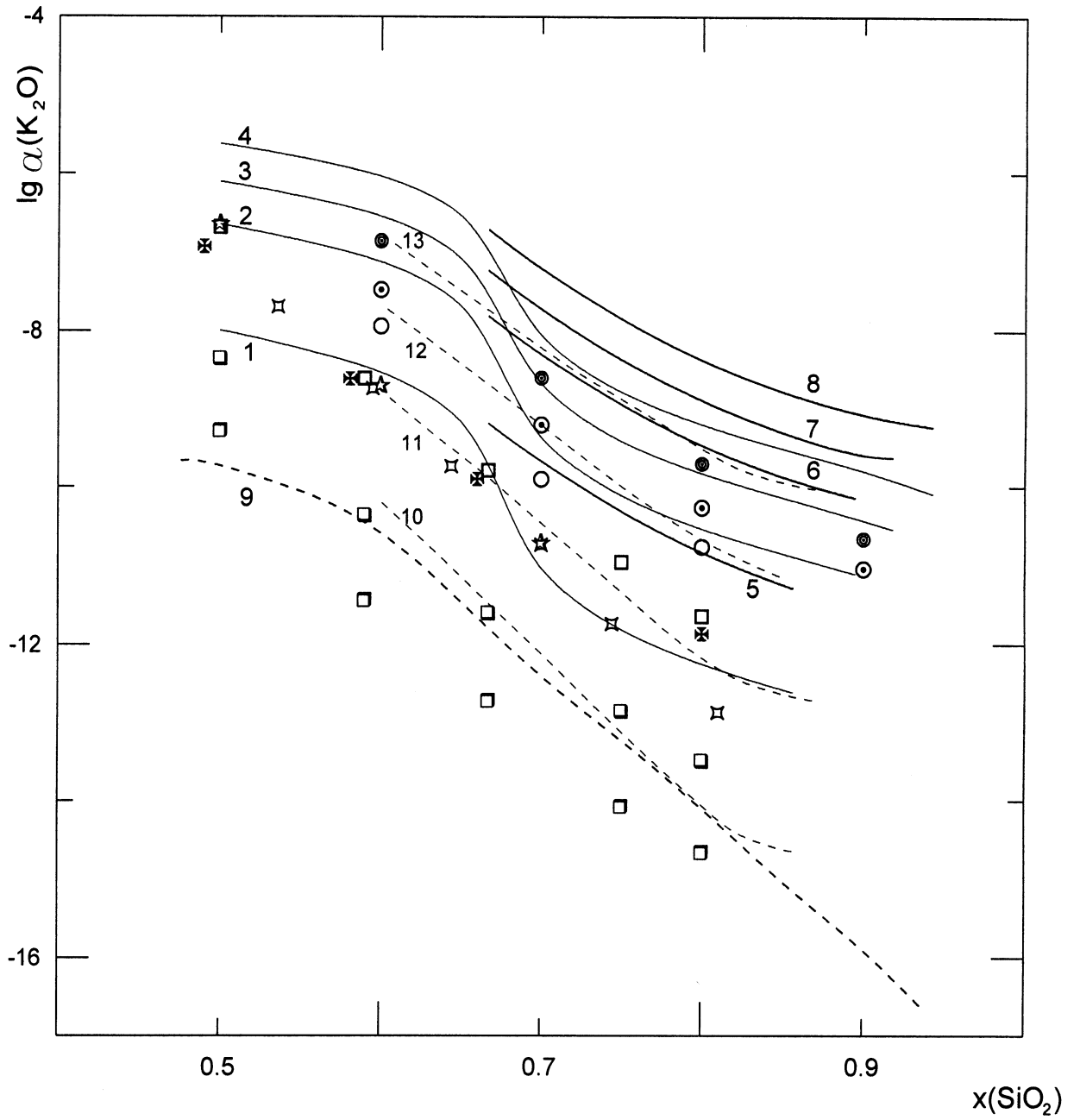


Figure 2. Comparison of  $K_2O$  activities in the  $K_2O$ - $SiO_2$  melt obtained in the present investigation [(1) 1373 K, (2) 1573 K, (3) 1673 K, (4) 1773 K] with the values available in the literature. Ref.[24]: (5) 1373 K, (6) 1573 K, (7) 1673 K, (8) 1773 K; ref. [10]: (9) 1273 K; ref. [42]: (10) 1273 K, (11) 1473 K, (12) 1673 K, (13) 1873 K; ref. [25]: ○ 1573 K, ⊙ 1673 K, ⊗ 1773 K; ref. [11]: ⋈ 1373; ref. [23]: ✕ 1318 K; ref. [21]: ☆ 1373 K; ref. [12]: □ 1373K, ◻ 1273 K, ◻ 1173 K.



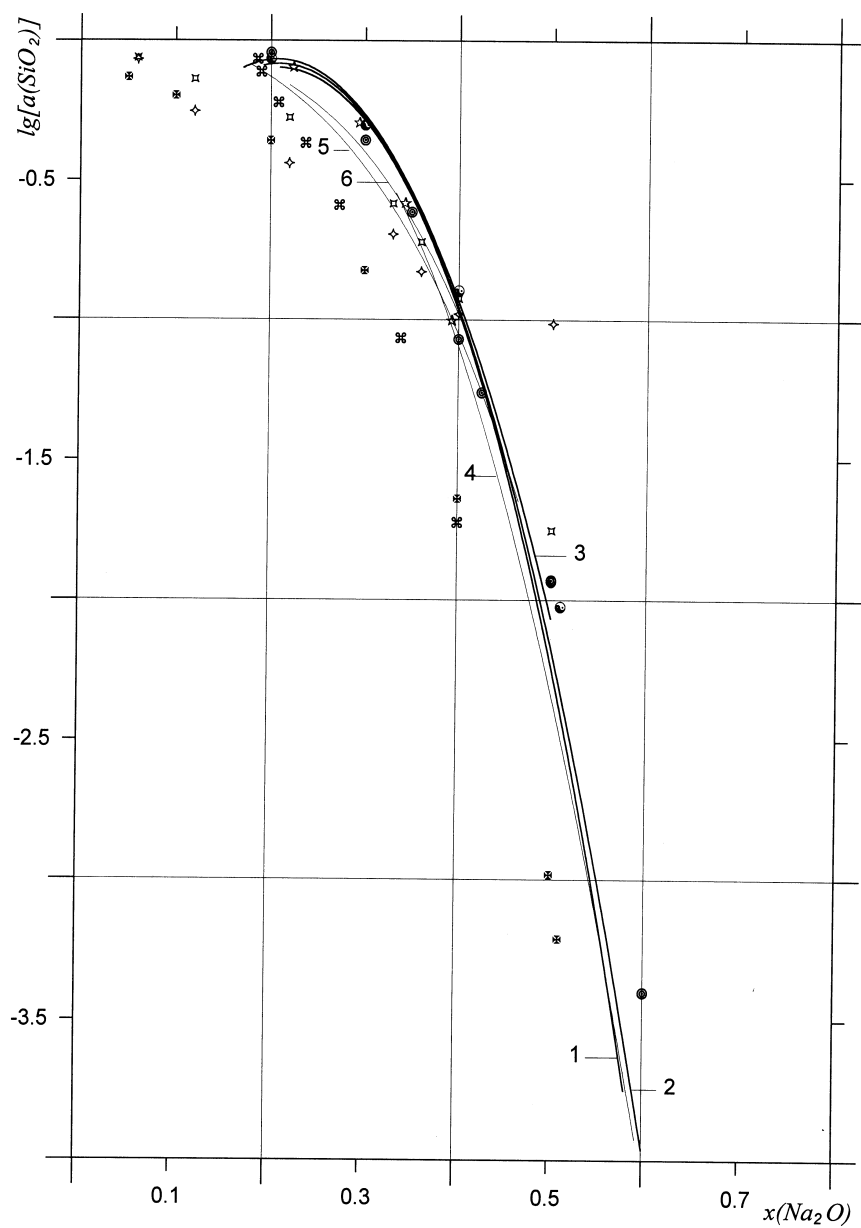


Figure 3. Comparison of  $\text{SiO}_2$  activities in the  $\text{Na}_2\text{O}$ - $\text{SiO}_2$  melt obtained in the present investigation [(1) 1373 K, (2) 1473 K, (3) 1573 K] with the values available in the literature. Ref. [18]: (4) 1473; ref. [2]: (5) 1573 K, (6) 1673 K; ref. [11]:  $\otimes$  1473 K; ref. [4]:  $\star$  1323 K; ref. [5]:  $\otimes$  1073 K,  $\square$  1473 K; ref. [1]:  $\odot$  1573 K, ref. [20]:  $\diamond$  1293 K,  $\nabla$  1423 K.

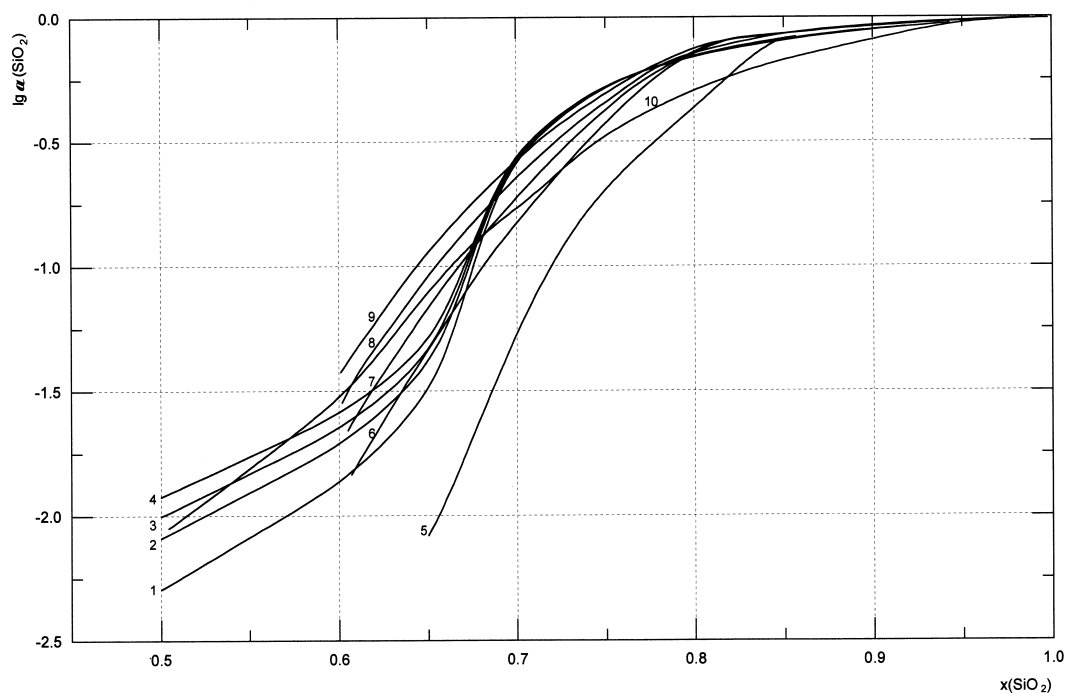


Figure 4. Comparison of  $\text{SiO}_2$  activities in the  $\text{K}_2\text{O}$ - $\text{SiO}_2$  melt obtained in the present investigation [(1) 1373 K, (2) 1573 K, (3) 1673 K, (4) 1773 K] with the values available in the literature. Ref. [11]: (5) 1373 K; ref. [42]: (6) 1273 K, (7) 1473 K, (8) 1673 K, (9) 1873 K; ref. [10]: (10) 1273 K.

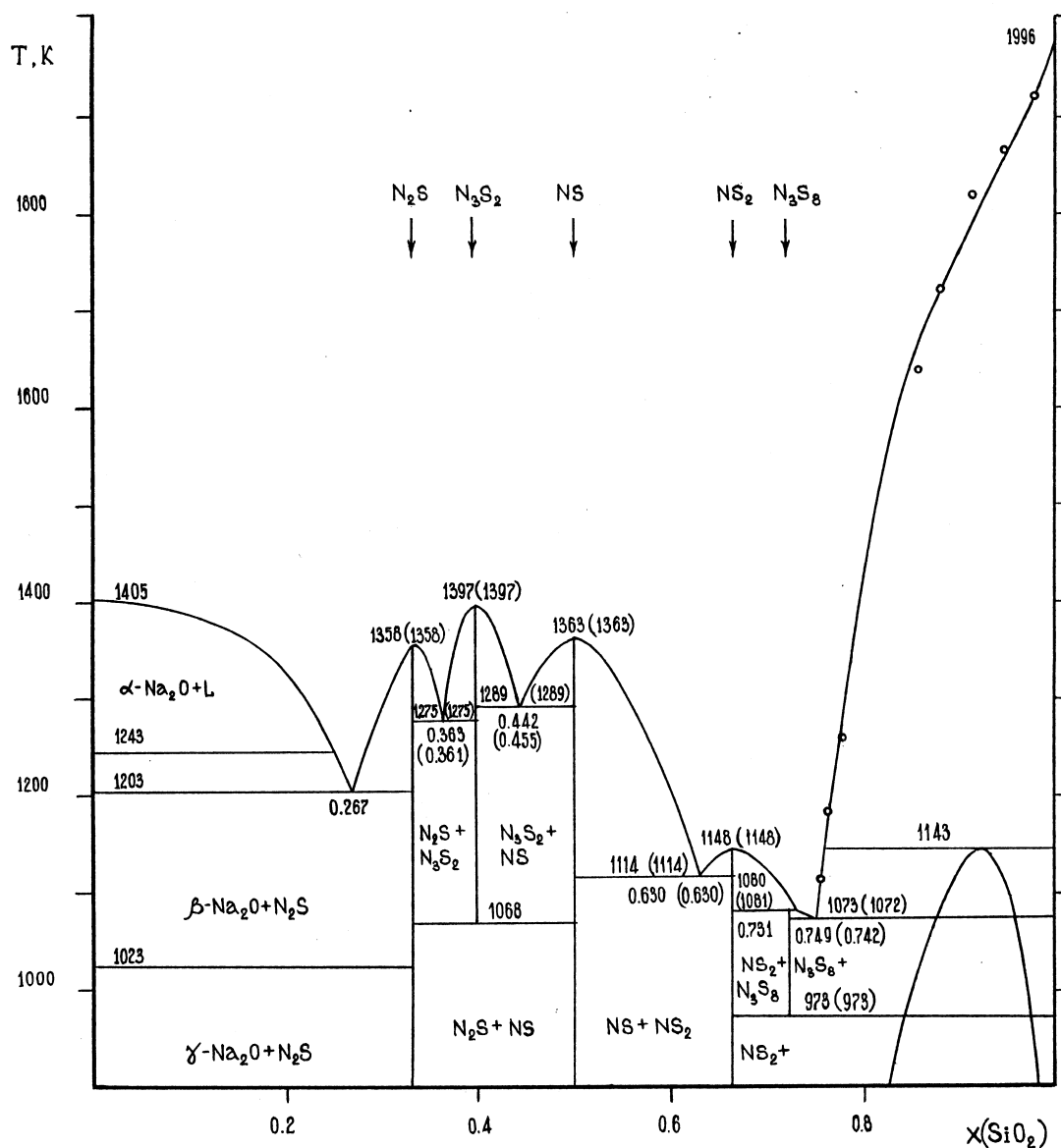


Figure 5. Phase diagram of the  $\text{Na}_2\text{O}-\text{SiO}_2$  system: solid lines, result of the present computation; data points, experimental data [48] on the line of saturation of the melt with  $\text{SiO}_2$ . Co-ordinates of the particular points: without parenthesis=present results, in parenthesis=data [48-52].

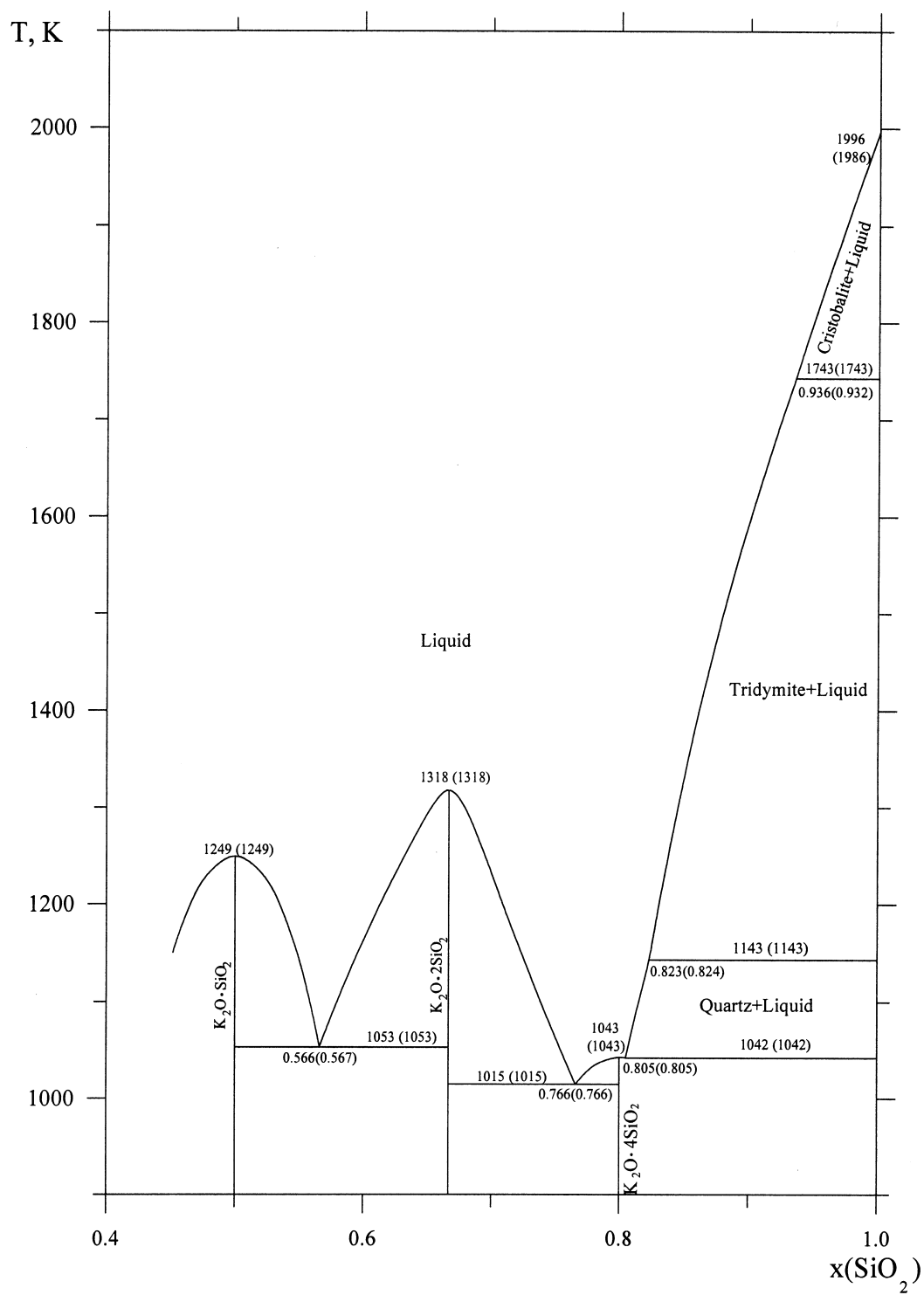


Figure 6. Phase diagram of the  $K_2O-SiO_2$  system. Co-ordinates of the particular points: without parenthesis=present results, in parenthesis=data [40].

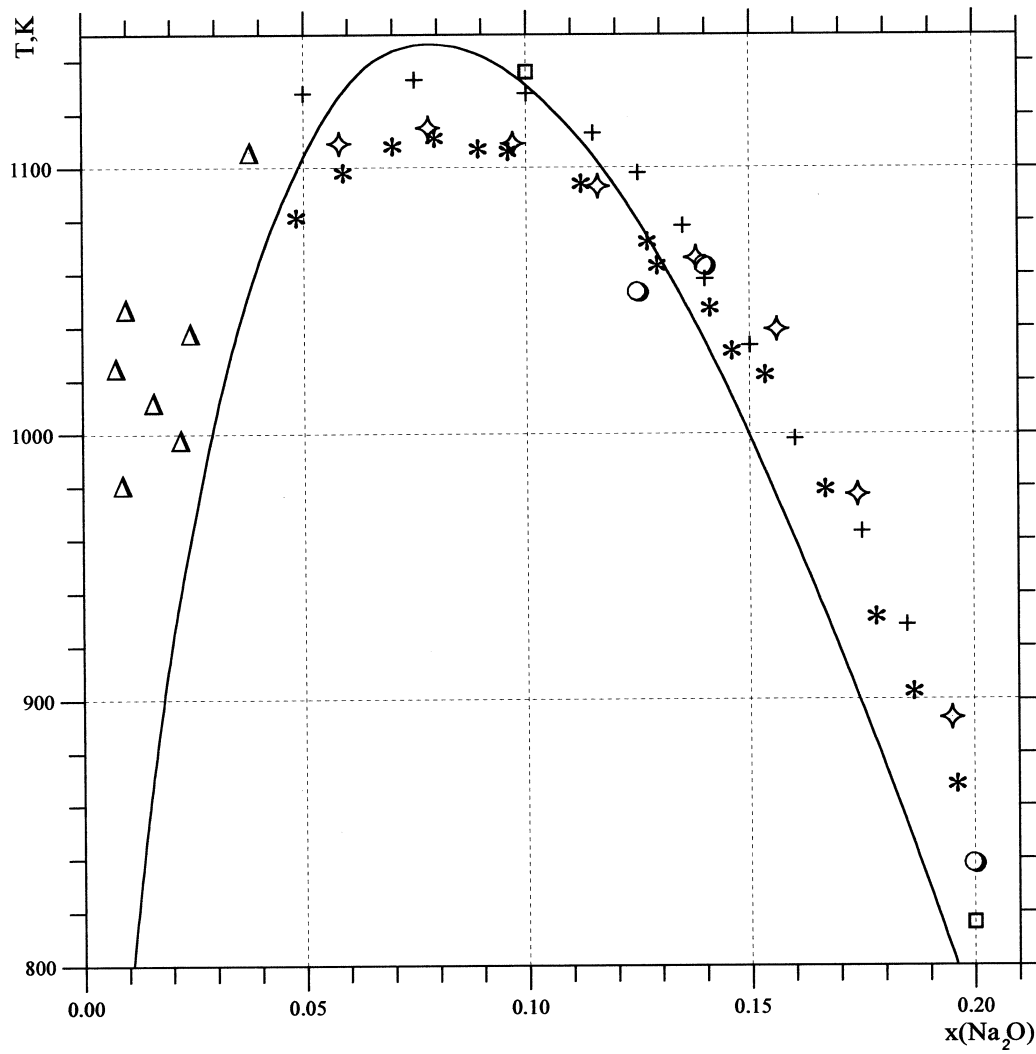


Figure 7. Immiscibility region in the liquid phase of the Na<sub>2</sub>O-SiO<sub>2</sub> system: solid line, result of the present computation; \*, ref. [60]; □, ref. [57]; +, ref. [54]; ◇, ref. [56]; O, ref. [55]; Δ, ref. [58].

Table 1. Comparison of experimentally obtained activities of Na<sub>2</sub>O, K<sub>2</sub>O and SiO<sub>2</sub> in the Na<sub>2</sub>O-SiO<sub>2</sub> and K<sub>2</sub>O-SiO<sub>2</sub> melts chosen at random with the activities calculated by means of the associated-solution model (reference states are liquid Na<sub>2</sub>O, K<sub>2</sub>O and SiO<sub>2</sub>).

$x$ (SiO <sub>2</sub> )	T/K	$a$ (SiO <sub>2</sub> )		$a$ (Me <sub>2</sub> O)	
		exp.	model	exp.	model
Na <sub>2</sub> O-SiO <sub>2</sub>					
0.805	1473	0.860	0.854	7.19×10 <sup>-10</sup>	7.13×10 <sup>-10</sup>
0.753	1273	0.735	0.729	5.29×10 <sup>-11</sup>	5.35×10 <sup>-11</sup>
0.709	1673	0.536	0.537	3.24×10 <sup>-8</sup>	3.24×10 <sup>-8</sup>
0.671	1173	0.342	0.337	4.67×10 <sup>-11</sup>	4.72×10 <sup>-11</sup>
0.625	1573	0.199	0.196	7.63×10 <sup>-8</sup>	7.65×10 <sup>-8</sup>
0.573	1473	0.0703	0.0698	1.02×10 <sup>-7</sup>	1.01×10 <sup>-7</sup>
0.524	1573	0.0204	0.0201	1.53×10 <sup>-6</sup>	1.56×10 <sup>-6</sup>
0.477	1373	1.75×10 <sup>-3</sup>	1.77×10 <sup>-3</sup>	1.32×10 <sup>-6</sup>	1.31×10 <sup>-6</sup>
0.430	1473	3.80×10 <sup>-4</sup>	3.83×10 <sup>-4</sup>	1.83×10 <sup>-5</sup>	1.83×10 <sup>-5</sup>
0.405	1423	1.38×10 <sup>-4</sup>	1.40×10 <sup>-4</sup>	2.01×10 <sup>-5</sup>	1.98×10 <sup>-5</sup>
0.382	1383	4.76×10 <sup>-5</sup>	4.73×10 <sup>-5</sup>	2.43×10 <sup>-5</sup>	2.44×10 <sup>-5</sup>
0.349	1373	3.77×10 <sup>-6</sup>	3.80×10 <sup>-6</sup>	8.62×10 <sup>-5</sup>	8.55×10 <sup>-5</sup>
K <sub>2</sub> O-SiO <sub>2</sub>					
0.892	1723	0.880	0.878	8.981×0 <sup>-11</sup>	8.92×10 <sup>-11</sup>
0.848	1573	0.808	0.809	1.45×10 <sup>-11</sup>	1.47×10 <sup>-11</sup>
0.811	1173	0.745	0.737	2.50×10 <sup>-15</sup>	2.47×10 <sup>-13</sup>
0.770	1073	0.597	0.601	1.87×10 <sup>-16</sup>	1.87×10 <sup>-16</sup>
0.722	1323	0.381	0.384	1.15×10 <sup>-12</sup>	1.14×10 <sup>-12</sup>
0.722	1673	0.389	0.394	8.80×10 <sup>-10</sup>	8.71×10 <sup>-10</sup>
0.674	1373	0.101	0.101	7.54×10 <sup>-11</sup>	7.41×10 <sup>-11</sup>
0.630	1323	1.87×10 <sup>-2</sup>	1.90×10 <sup>-2</sup>	5.84×10 <sup>-10</sup>	5.77×10 <sup>-10</sup>
0.630	1523	2.67×10 <sup>-2</sup>	2.64×10 <sup>-2</sup>	2.01×10 <sup>-8</sup>	1.98×10 <sup>-8</sup>
0.591	1323	1.11×10 <sup>-2</sup>	1.12×10 <sup>-2</sup>	1.35×10 <sup>-9</sup>	1.33×10 <sup>-9</sup>
0.543	1473	9.69×10 <sup>-3</sup>	9.61×10 <sup>-3</sup>	3.50×10 <sup>-8</sup>	3.48×10 <sup>-8</sup>
0.500	1473	6.44×10 <sup>-3</sup>	6.52×10 <sup>-3</sup>	5.38×10 <sup>-8</sup>	5.32×10 <sup>-8</sup>

Table 2. Thermodynamic functions of formation of sodium and potassium silicates from  $\beta$ - $\text{Na}_2\text{O}$ , solid  $\text{K}_2\text{O}$  and quartz.

Silicate	Temperature range, K	$-\Delta H / \text{J mol}^{-1}$	$\Delta S / \text{J mol}^{-1} \text{K}^{-1}$
1/11 $3\text{Na}_2\text{O} \cdot 8\text{SiO}_2$	974-1071	58300 $\pm$ 755	6.70 $\pm$ 0.70
1/3 $\text{Na}_2\text{O} \cdot 2\text{SiO}_2$	973-1078	73660 $\pm$ 715	5.70 $\pm$ 0.70
1/2 $\text{Na}_2\text{O} \cdot \text{SiO}_2$	953-1110	115400 $\pm$ 600	-2.30 $\pm$ 0.60
1/5 $3\text{Na}_2\text{O} \cdot 2\text{SiO}_2$	1068-1285	110500 $\pm$ 580	6.15 $\pm$ 0.55
1/3 $2\text{Na}_2\text{O} \cdot \text{SiO}_2$	942-1271	127100 $\pm$ 620	-6.90 $\pm$ 0.60
1/5 $\text{K}_2\text{O} \cdot 4\text{SiO}_2$	891-1041	65900 $\pm$ 500	1.18 $\pm$ 0.41
1/3 $\text{K}_2\text{O} \cdot 2\text{SiO}_2$	869-1014	112560 $\pm$ 540	-3.47 $\pm$ 0.50
1/2 $\text{K}_2\text{O} \cdot \text{SiO}_2$	879-1050	145940 $\pm$ 570	-5.24 $\pm$ 0.57

Table 3. Standard thermodynamic functions of solid silicates.

Silicate	Source	$S_{298.15}^\circ$ $\text{J mol}^{-1} \text{K}^{-1}$	Formation from oxides		Formation from elements
			$-\Delta_f H / \text{kJ mol}^{-1}$	$-\Delta_f S / \text{J mol}^{-1} \text{K}^{-1}$	$-\Delta_f H / \text{kJ mol}^{-1}$
$\text{Na}_2\text{O} \cdot 2\text{SiO}_2$	present	165.4 $\pm$ 4.0	227.4 $\pm$ 5	7.3 $\pm$ 3.0	2464.2
	[26]	164.055	230.54	6.03	2467.3
$\text{Na}_2\text{O} \cdot \text{SiO}_2$	present	114.8 $\pm$ 3.0	228.1 $\pm$ 5	-1.7 $\pm$ 2.0	1554.0
	[26]	113.805	230.12	-2.76	1556.03
$2\text{Na}_2\text{O} \cdot \text{SiO}_2$	present	194.1 $\pm$ 5.0	363.0 $\pm$ 8	2.4 $\pm$ 4.0	2104.0
	[26]	195.811	359.8	4.15	2100.8
$\text{K}_2\text{O} \cdot 4\text{SiO}_2$	present	260.0 $\pm$ 7.0	324.7 $\pm$ 9.0	0.0 $\pm$ 6.0	4329.6
	[26]	265.684	309.616	5.70	4314.545
$\text{K}_2\text{O} \cdot 2\text{SiO}_2$	present	184.1 $\pm$ 5.0	325.6 $\pm$ 7.0	7.0 $\pm$ 4.0	2510.5
	[28]	182.004	324.26	4.90	2509.145
	[26]	190.581	326.352	13.52	2509.567
$\text{K}_2\text{O} \cdot \text{SiO}_2$	present	146.0 $\pm$ 4.0	277.7 $\pm$ 6.0	10.4 $\pm$ 3.0	1551.8
	[27]	146.147	274.061	10.54	1548.089
	[26]	146.147	317.984	10.55	1590.346